The 2022 WMO Technical Conference on Meteorological and Environmental Instruments and Methods of Observation (TECO-2022)

10-13 October 2022, Paris (France)

WIND TUNNEL VALIDATION OF A PARTICLE TRACKING MODEL TO EVALUATE THE WIND-INDUCED BIAS ON RAINFALL MEASUREMENTS

Arianna Cauteruccio[1,3]; Elia Brambilla[2]; Mattia Stagnaro [1,3]; Luca G. Lanza[1,3]; Daniele Rocchi[2]

[1] Department of Civil, Chemical and Environmental Engineering, University of Genova, Genova, Italy

[2] Department of Mechanical Engineering, Politecnico di Milano, Milan, Italy

[3] WMO Lead Centre on Precipitation Intensity, Genova, Italy

Corresponding author: Arianna Cauteruccio, arianna.cauteruccio@edu.unige.it

Abstract:

Precipitation measurements obtained by employing catching-type precipitation gauges are affected by biases due to the wind-gauge body interaction, which affects hydrometeor trajectories and the collection performance. This topic can be investigated by using CFD simulations which provide the airflow field surrounding the gauge body and a Lagrangian Particle Tracking (LPT) model to assess the influence of the airflow deformation on the hydrometeor trajectories. In this work, a literature LPT model, used for snow particles, was modified by introducing drag coefficient equations suitable for rain. Within the activities of the PRIN 20154WX5NA project, with the aim to validate the LPT model, a dedicated setup was realized in the Politecnico di Milano Wind Tunnel (WT) able to release water drops and to detect their deviation when approaching the gauge and traveling above the collector. The more traditional shapes of catching-type gauges were tested. A high-speed camera and a high-power lamp were used to capture and illuminate drops along their trajectories. The validation was obtained by comparison between observed and simulated trajectories. In the numerical model, the initial conditions (position and velocity) of the simulated trajectories were set consistently with the WT observations. The observed trajectories closely reproduce the modelled ones therefore validating the numerical model and confirming that the formulation used for the drag coefficient is suitable to reproduce the observed behaviour of the hydrometeors when affected by the airflow deformation due to the bluff-body aerodynamics of precipitation gauges. Furthermore, the deviated trajectories of the observed drops allowed to clearly visualize the wind-induced undercatch of catching-type precipitation gauges.

1. Introduction

The wind-induced undercatch of catching type precipitation gauges is defined as the reduced amount of precipitation captured by the collector of the gauge with respect to the amount that would be captured if the gauges were transparent to the wind. When any gauge is exposed to the wind, airflow deformations occur above and upwind of the collector due to the bluff-body aerodynamics of the gauge outer geometry. Significant acceleration and vertical velocity components are generated (see e.g., Warnik, 1953), inducing some

deformation of the fall trajectories of the approaching hydrometeors and generally resulting in a lower collection of precipitation than in the absence of wind.

Adjustments for the wind-induced bias are traditionally derived from field experiments (see e.g., Wolff et al., 2015), where the ratio between the precipitation amount measured by the gauge and a suitable reference configuration with limited exposure to the wind is used as a measure of the Collection Efficiency (CE). This is a function of the wind speed at the collector's height and of further influencing variables, such as the microphysical characteristics of the precipitation events at the field test site.

Most recent advances in the literature are concentrated on a physically based numerical approach (see Colli et al. 2016 a,b) to supplement experimental studies. The numerical approach is based on Computational Fluid Dynamics (CFD) simulations of the airflow field surrounding the gauge body (see e.g., Colli et al., 2018) and a Lagrangian Particle Tracking (LPT) model to evaluate the airflow induced deformation on the trajectory of the approaching hydrometeors (see e.g., Nešpor & Sevruk, 1999).

Colli et al. (2015) provided an improvement of the trajectory model obtaining a better comparison between numerical results and real-world data by introducing the dependence of the aerodynamic Drag Coefficient (CD) on the local Reynolds number of the simulated particle (Re_p).

In the present work, the LPT model used by Colli et al. (2015) for solid precipitation was adapted to simulate the trajectories of water drops when falling through the atmosphere and approaching the gauge collector, using suitable CD equations as a function of the Re_p. Various equations were implemented for different Re_p ranges derived from literature formulations and data. A dedicated wind tunnel (WT) experimental setup was developed, where a physical full-scale model was designed and realized to release water drops in the flow field and to detect — with a high resolution — their deviated trajectories close to the gauge collector, where the airflow field is modified by the presence of the gauge body. Various wind speed and fall height combinations were tested in a controlled WT environment. Flow velocity measurements were obtained by employing a multi-hole probe and a Particle Image Velocimetry (PIV) technique.

The objective of the present work is the validation in the WT of the modeling chain composed of CFD simulations— to establish the airflow patterns (acceleration, velocity components and turbulence intensity) produced by the aerodynamic response of the gauge geometry— and LPT algorithm to assess the one-way coupled airflow-raindrop interaction.

2. Methods

The validation of trajectory models is yet scarcely documented in the literature. Very few works, e.g., Warnik (1953) and Green and Helliwell (1972), report some attempts to detect water drops in the WT.

In the present work, the most popular outer shapes of catching type precipitation gauges, cylindrical (hereinafter CY) and chimney (CH) shapes, were investigated (see Figure 1).

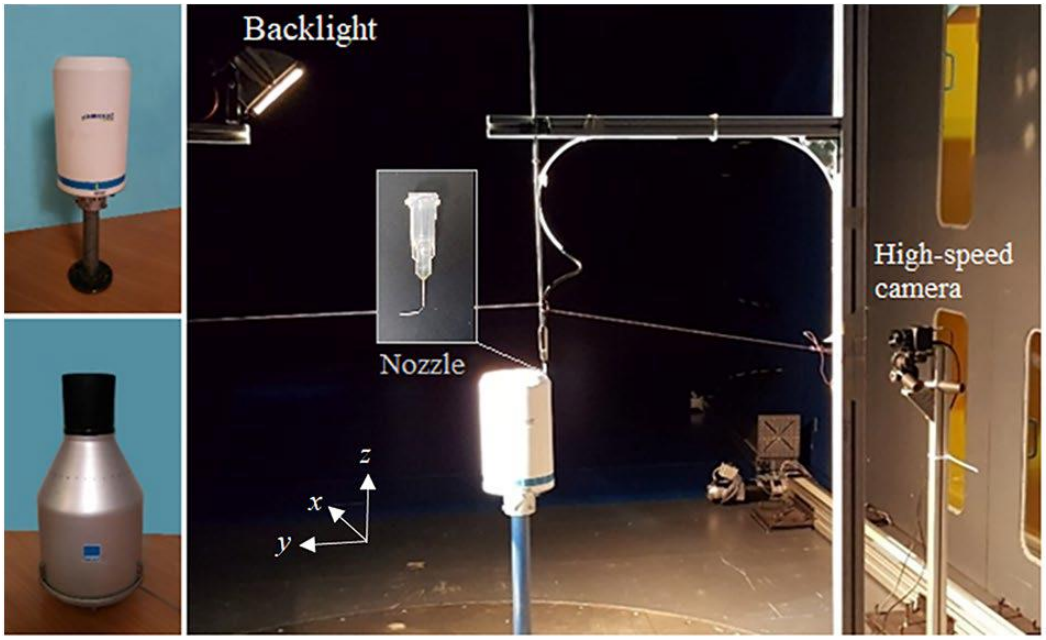

Figure 1: CY (top-left) and CH (bottom-left) precipitation gauges and experimental setup used to release drops and take photographs of their trajectories as installed in the GVPM (wind is along the x direction). [Source : Cauteruccio, et al. 2021a]

An extensive experimental campaign was conducted in the WT of the DICCA department at the University of Genova and in the WT facility available at Politecnico di Milano, hereafter GVPM. This includes flow velocity measurements obtained by using a multi-hole probe (employed in the DICCA WT), as well as Particle Image Velocimetry (PIV) and a dedicated technique designed to release and track water drops using a drop generator and a high-speed camera (employed in the GVPM).

Dedicated numerical simulations of the experimental setup were performed with suitable initial conditions (drop velocity and position), as observed in the WT. The comparison between CFD airflow fields and velocity measurements and between the simulated and observed drop trajectories led to the validation of the whole numerical approach.

The DICCA WT has a working chamber 8.8 m long, with a cross area of 1.7 × 1.35 m^2 (width × height), while the GVPM has a low turbulence-high speed chamber of 4 × 4 × 4 m^3. In both facilities the gauge collectors were positioned at 1 m from the floor and in the center of the cross section to avoid any interaction with the surrounding walls. The CY gauge was tested in the DICCA WT. Measurements of the wind speed were acquired using a fast-response multi-hole probe, the "Cobra" probe, characterized by a measuring cone of ±45°, mounted on a traversing system with three degrees of freedom. Each measurement was sampled at 2 kHz for 30 s. The CH gauge was tested in the GVPM using the PIV technique. The test chamber was uniformly filled with castor oil smoke, used as a tracer. A laser emitter was mounted on the ceiling of the test chamber to illuminate the measurement plane, while the surrounding environment was kept in the dark. The video camera was positioned with its central axis normal to the streamwise direction (x) and

centered on the gauge collector. Post processing of the acquired images provided the flow velocity field discretized in a regular grid with cell size of 7.5 × 7.5 mm. With the aim to validate the LPT model, water drops were injected in the GVPM and their trajectories were captured with a high-speed camera in the vertical 2-D plane (x, z) along the main flow direction. The deviation of the drop trajectories approaching and traveling above the gauge collector was measured. The WT was equipped with a hydraulic system and a high-power lamp to generate and illuminate drops along their trajectories. The experimental setup is illustrated in Figure 1. During the experiment drops of diameter between 0.7 and 1.2 mm were generated. The videos recorded by the camera were analyzed and filtering algorithm were applying to extract the middle line streak from the image, directly corresponding to the trajectory of the drop.

The LPT model used by Colli et al. (2015) for solid precipitation was modified by introducing drag coefficient equations, as a function of R_{ep}, suitable for liquid precipitation. Folland (1988) proposed the following relationships between R_{ep} and CD, for various ranges of Rep and assumed that the minimum value for CD must be fixed at 0.55:

$$Re_p < 0.01 \quad C_D = 2547$$

$$0.01 \le Re_p < 2 \quad C_D = 1.06\left(24\, Re_p^{-1} + 2.400\, Re_p^{-0.045}\right)$$

$$2 \le Re_p \le 21 \quad C_D = 1.06\left(24\, Re_p^{-1} + 2.640\, Re_p^{-0.190}\right)$$

$$21 < Re_p \quad C_D = 1.06\left(24\, Re_p^{-1} + 4.536\, Re_p^{-0.368}\right)$$

In the work of Khvorostyanov and Curry (2005) (hereinafter KC05), different formulations of CD, as a function of R_{ep} obtained from experimental studies and analytical models, were summarized. The CD values proposed by KC05 as a function of Rep, for spherical particles in turbulent conditions, were fitted here for Rep > 60 with an inverse first-order equation:

$$C_D = y_0 + \frac{(ab)}{b + Re_p}$$

where the values obtained for the three parameters are y_0 = 0.442, a = 3.402, b = 21.383 and the correlation factor (R^2) is equal to 0.996.

As shown in Figure 2, also the relationships proposed by Folland (1988) (black line) were compared with the raw data provided by KC05 (diamond). Based on this comparison the proposed best-fit curve (gray line in Figure 2) was implemented in the LPT model to calculate the drag coefficient for Rep > 400, while the equations proposed by Folland (1988) were adopted for Rep ≤ 400.

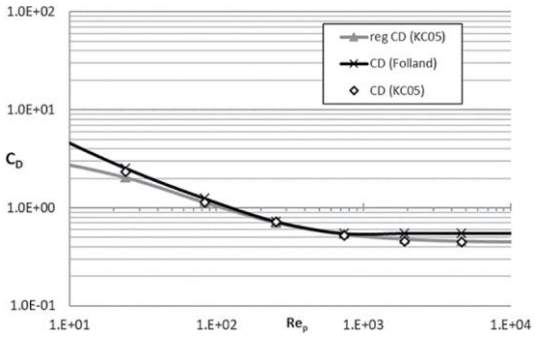

Figure 2: Comparison between the raw data provided by KC05 (diamond), the proposed best-fit curve (gray line) and the formulation by Folland (1988) (black line). [Source: Cauteruccio et al. 2021a]

The LPT model was applied to the simulated airflow field to reproduce the trajectories of water drops as released in the WT. These were compared to the trajectories of the real drops detected by means of the video tracking system installed in the WT.

3. Results and discussion

The validation of the LPT model was obtained by comparison between observed and simulated trajectories. In the numerical model the initial conditions, normalized position (x/D and z/D) and velocity components (u and w [m s^{-1}], the latter assumed positive downward), of the simulated trajectories were set consistently with the WT observations. CFD airflow velocity fields were rescaled according to the free-stream velocity value used in the WT. The initial velocity components were set equal to the mean values of the three to five initial positions of each drop as shot by the camera, to avoid the noise due to the uncertainty in the initial positions. The drop diameter, d, which has a major role in the calculation of the drop trajectory by affecting Re_p and therefore CD, is obtained here as a calibration parameter for each trajectory, since the drop releasing mechanism and the acquisition system cannot provide sufficient accuracy in the assessment of the drop size.

A sample of 25 observed drop trajectories is compared with the simulated ones to support the validation phase. They were chosen to cover a variety of wind speed, drop size, initial drop velocity and position for each gauge geometry.

The observed (circles) and simulated (solid line) patterns of the drop trajectory identified with the name G2, are compared in Figure 3. The maximum difference between the vertical positions (z in mm), computed at each normalized longitudinal coordinate (x/D) of the observed trajectory, arises at the upwind edge of the collector and is about 1.2 mm. This difference is comparable with the drop size, therefore with the uncertainty in the assessment of the drop position, identified as a bright moving object in each frame. The calculated horizontal acceleration of the drop, normalized with the one experienced in the initial undisturbed part of the trajectory, is also shown (scale on the right-hand axis). Consistently with the PIV airflow velocity fields (see Cauteruccio et al. 2021 a,b), the drop significantly accelerates when traveling above the upwind part of the collector, where the airflow is indeed accelerated, until crossing the separation layer between the airflow recirculation and accelerated zones, when it starts decelerating abruptly toward the downwind edge of the collector.

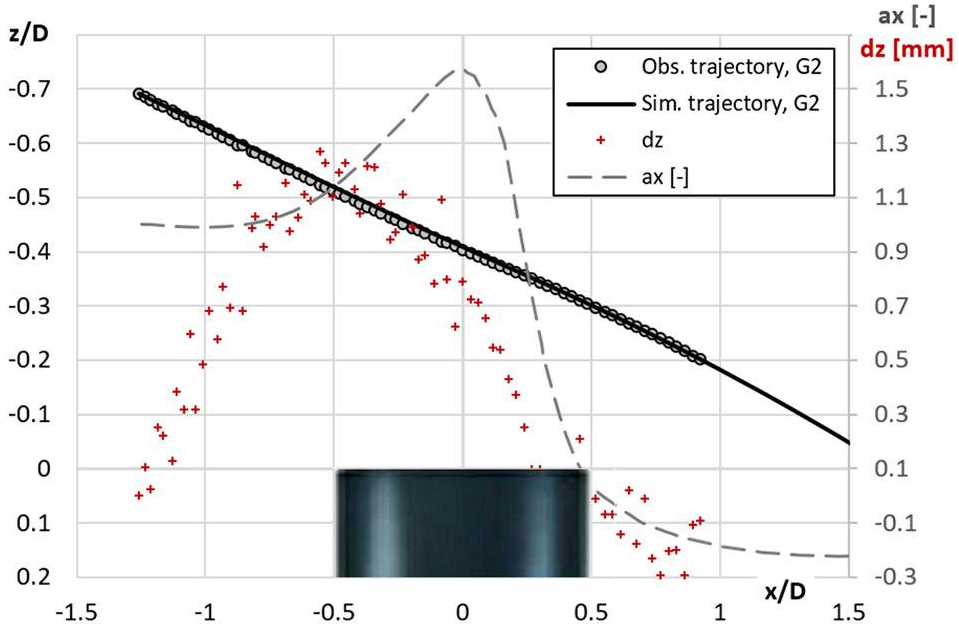

Figure 3: Observed (circles) and simulated (solid line) drop trajectories above the collector of the CH gauge at a wind speed equal to 10.2 m s^{-1}. The difference dz (mm) between the observed and simulated vertical coordinates of the drop trajectories (red crosses) at each normalized observed longitudinal coordinate (x/D) is reported (scale on the right-hand axis), together with the numerical longitudinal acceleration (a_x) of the drop (dashed line). [Source: Cauteruccio et al. 2021]

The good repeatability of the trajectories of very similar drops in the WT is shown in Figure 4. By injecting drops of the same size in the WT, the observed trajectories are indeed very close to each other, and they experience very similar deviations above the collector. Moreover, simulated trajectories show that the LPT model is able to replicate even the small variations due to slight differences in the initial conditions about the drop velocity.

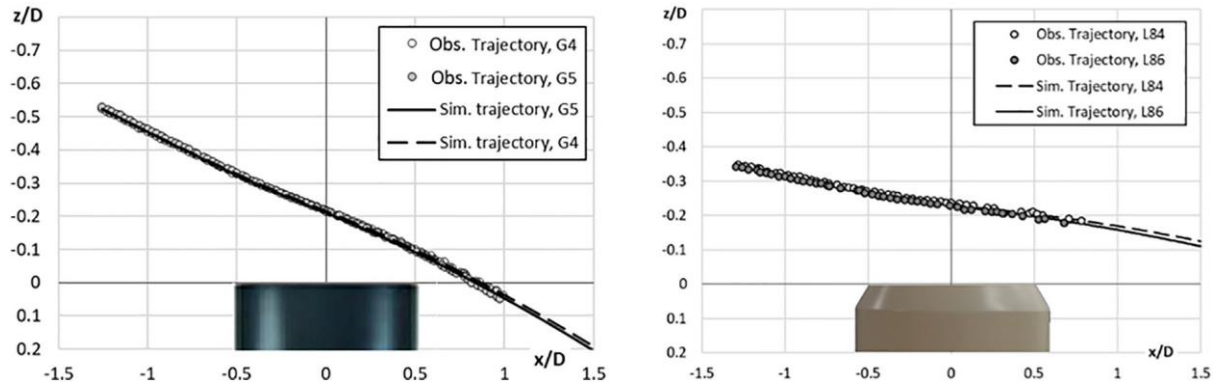

Figure 4: Pairs of drops having approximately the same size traveling above the collector of the CH gauge at wind speed equal to 10.2 m s^{-1} (left-hand panel) and CY gauge at 13.1 m s−1 (right-hand panel). Observed (circles) and simulated (lines) trajectories are depicted for the two pairs of drops. [Source: Cauteruccio et al. 2021]

Validation of the coupled CFD and LPT approach was obtained after numerically simulating about 25 trajectories of drops released in the WT experiment. A synthesis of the validation performance is reported in Table 1. The maximum, mean and median difference, dz, between the vertical coordinates along each observed and simulated trajectory, normalized with the estimated drop diameter, d, were calculated as suitable performance parameters. For each of them, the maximum, minimum, mean and standard deviation values obtained over the set of all trajectories used in the validation exercise are listed in the table. The same statistics are included for the root mean square difference (RMSD) between the observed and simulated vertical coordinates along each trajectory.

Table 1: Validation Statistics for the Selected Performance Parameters [Source: Cauteruccio et al. 2021a]

		Max (dz/d)	**Mean (dz/d)**	**Median (dz/d)**	**RMSD**
Max		2.1492	1.0444	1.2154	0.000812
Min		0.1871	−0.4230	−0.4946	0.000213
Mean		1.0968	0.0332	0.0337	0.000429
Std. Dev.		0.4351	0.3514	0.3905	0.000168

The validation was satisfactory since the mean of the maximum normalized differences between the simulation and the observed trajectory is about unity, with a low standard deviation (the coefficient of variation is about 0.4). Also, the mean and median values of dz are very similar, showing a symmetrical spread of these differences around the perfect agreement, which suggests quite a random nature of the error. Finally, the RMSD is very low, always below 10^{-3}, indicating an overall good agreement for all pairs of simulated and observed trajectories.

4. Conclusions

The present work sheds additional light on the wind exposure problem, with results that can be used operationally to adjust precipitation measurements obtained in windy conditions. Indeed, the WT validation of the numerical approach based on CFD and LPT simulations supports its use as the theoretical basis for the interpretation of the wind-induced bias of field measurements obtained from shielded and unshielded precipitation gauges.

Typical applications include the numerical calculation of the collection efficiency of precipitation gauges having different outer geometries (based on suitable assumptions and/or ancillary measurements about the hydrometeor characteristics, drag coefficient and drop size distribution). Adjustment curves for the wind-induced bias of precipitation measurements can be therefore derived to be used operationally for correcting the raw measurements (Cauteruccio and Lanza, 2020).

Also, this work may help investigating the propagation of measurement biases into the modeling of hydrological processes, especially in the field of water resources assessment, by validating a suitable simulation framework. Fully validated simulations are indeed precious to quantify the impact of wind-induced errors on the estimation of rain fields used as an input to hydrological models operating at the natural catchment scale.

Additionally, knowledge of the wind-induced biases of ground-based measurement instruments supports a better understanding of the reliability of remotely sensed estimates of the rain field from satellite sensors, which provide the necessary information about areal precipitation over large regions, and of the uncertainty of radar-based rainfall retrieval.

Both such aspects were the focus of an Italian national project entitled "Reconciling precipitation with runoff: the role of understated measurement biases in the modeling of hydrological processes," which raised the need for the present research.

5. References

Cauteruccio, A., Brambilla, E., Stagnaro, M., Lanza, L.G. and D. Rocchi (2021a). Wind tunnel validation of a particle tracking model to evaluate the wind-induced bias of precipitation measurements. *Water Resour. Res.,* **57**(7), e2020WR028766. https://doi.org/10.1029/2020WR028766

Cauteruccio, A., Brambilla, E., Stagnaro, M., Lanza, L.G. and D. Rocchi (2021b). Experimental evidence of the wind-induced bias of precipitation gauges using Particle Image Velocimetry and particle tracking in the wind tunnel. *J. of Hydrol.,* **600**, 126690. https://doi.org/10.1016/j.jhydrol.2021.126690

Cauteruccio, A. and L.G. Lanza (2020). Parameterization of the collection efficiency of a cylindrical catching-type rain gauge based on rainfall intensity. *Water*, **12**(12), 3431. https://doi.org/10.3390/w12123431

Colli, M., Lanza, L. G., Rasmussen, R., & Thériault, J. M. (2016a). The collection efficiency of shielded and unshielded precipitation gauges. Part I: CFD airflow modelling. *J. of Hydrometeorol*., **17**, 231–243. https://doi.org/10.1175/JHM-D-15-0010.1

Colli, M., Lanza, L. G., Rasmussen, R., & Thériault, J. M. (2016b). The collection efficiency of unshielded precipitation gauges. Part II: Modeling particle trajectories. *J. of Hydrometeorol.*, **17**, 245–255. https://doi.org/10.1175/JHM-D-15-0011.1

Colli, M., Lanza, L. G., Rasmussen, R., Thériault, J. M., Baker, B. C., & Kochendorfer, J. (2015). An improved trajectory model to evaluate the collection performance of snow gauges. J. Appl. Meteorol. Climatol., **54**, 1826–1836. https://doi.org/10.1175/JAMC-D-15-0035.1

Colli, M., Pollock, M., Stagnaro, M., Lanza, L. G., Dutton, M., & O'Connell, P. E. (2018). A Computational Fluid-Dynamics assessment of the improved performance of aerodynamic raingauges. *Water Resour. Res.*, **54**, 779–796. https://doi.org/10.1002/2017WR020549

Folland, C. K. (1988). Numerical models of the raingauge exposure problem, field experiments and an improved collector design. *Quarterly Journal of the Royal Meteorological Society*, **114**, 1485–1516. https://doi.org/10.1002/qj.49711448407

Green, M. J., & Helliwell, P. R. (1972). The effect of wind on the rainfall catch. Distribution of precipitation in mountainous areas. World Meteorological Organization Report 326, 2, 27–46.

Khvorostyanov, V. I., & Curry, J. A. (2005). Fall velocities of hydrometeors in the atmosphere: Refinements to a continuous analytical power law. *Journal of the Atmospheric Sciences*, **62**, 4343–4357. https://doi.org/10.1175/JAS3622.1

Nešpor, V., & Sevruk, B. (1999). Estimation of wind-induced error of rainfall gauge measurements using a numerical simulation. *J. Atmos. Ocean. Technol.*, **16**(4), 450–464. https://doi.org/10.1175/1520-0426(1999)016%3C0450:EOWIEO%3E2.0.CO;2

Wolff, M.A.; Isaksen, K.; Petersen-Øverleir, A.; Ødemark, K.; Reitan, T.; Brækkan, R. (2015). Derivation of a new continuous adjustment function for correcting wind-induced loss of solid precipitation: Results of a Norwegian field study. *Hydrol. Earth Syst. Sci*., **19**, 951–967.

Warnik, C. C. (1953). Experiments with windshields for precipitation gages. *Transactions - American Geophysical Union*, **34**(3), 379–388. https://doi.org/10.1029/TR034i003p00379